

Quantitative study of grain refinement in Al–Mg alloy processed by equal channel angular pressing at cryogenic temperature

Y.J. Chen, H.J. Roven, S.S. Gireesh, P.C. Skaret, J. Hjelen

Department of Materials Science and Engineering, Norwegian University of Science and Technology, 7491 Trondheim, Norway

abstract

Strain induced grain refinement of an Al–1 wt.%Mg alloy processed by equal channel angular pressing (ECAP) at cryogenic temperature is investigated quantitatively. The results show that both mean grain and subgrain sizes are reduced gradually with increasing ECAP pass. ECAP at cryogenic temperature increases the rate of grain refinement by promoting the fraction of high angle grain boundaries (HAGBs) and misorientation at each pass. The fraction of HAGBs and the misorientation of Al–1 wt.% Mg alloy during ECAP at cryogenic temperature increase continuously as a function of equivalent strain. Both {110} and {111} twins at ultrafine-grained size are observed firstly in Al–Mg alloy during ECAP. The analysis of grain boundaries and misorientation gradients demonstrates the grain refinement mechanism of continuous dynamic recrystallization.

Keywords:

Al–Mg alloy
Electron backscattering diffraction (EBSD)
Severe plastic deformation (SPD)
Grain refinement
Microstructure
Grain boundaries

1. Introduction

Equal channel angular pressing (ECAP), one of the most promising severe plastic deformation (SPD) methods, has been widely applied for obtaining bulk ultrafine-grained (UFG) Al and its alloys. Much work has been done to minimize the grain size by optimizing the ECAP parameters [1–5]. It is well established that optimum processing by ECAP requires the lowest possible extrusion temperature and the highest accumulated strain (saturation strain). Increasing magnesium content in Al–Mg alloys, which decreases the stacking fault energy [2], normally results in smaller grain size [1,3,4]. However, crack and failure could occur when Al–Mg alloys containing more than 4 wt.% Mg are processed by ECAP at room temperature [5].

The aim of this study is thus to explore the possibility of Al–1 wt.% Mg alloy processed by ECAP at cryogenic temperature and analyze quantitatively the grain refinement during 1 to 4 passes of ECAP.

2. Experimental

Al–1 wt.% Mg alloy (Al–0.971 Mg, by wt.%) was chosen. Samples were received in the as-cast condition and were annealed to give an initial grain size of 960 μm . ECAP was performed with route Bc, using a 100 mm \times 19.5 mm \times 19.5 mm bar in a 90° die, which leads to an imposed strain of about 1.0 per pass. The die was kept at 243 K in a freezer for 8 h before ECAP and was surrounded by dry ice during ECAP to maintain the targeting temperature. All samples were kept in liquid

nitrogen for 30 min before and between each ECAP pass. Pairs of samples were pressed continuously and 1, 2, 3 and 4 ECAP passes were applied. After processing, the center of the longitudinal plane was prepared for electron backscattering diffraction (EBSD) analyses. EBSD mapping was done with a Zeiss Ultra 55 limited edition FEG-SEM.

3. Results and discussion

Fig. 1 shows the orientation maps and grain boundary maps obtained after 1, 2, 3 and 4 ECAP passes. In order to study the evolution of the grain boundaries in Fig. 1b, d and f, high angle grain boundaries (HAGBs), with misorientations in the range of 15–30° and above 30°, are marked with thick blue and black lines, respectively. The low angle grain boundaries (LAGBs), with misorientations in the range of 10–15° and 1.5–10°, are marked with thin blue and red lines, respectively. Fig. 1a and b show a clearly heterogeneous microstructure after the first pass of ECAP, with a mixture of elongated initial grains, deformation bands (DBs), new fine grains and a high fraction of subgrains. The thick blue boundaries (15–30°) are probably new grain boundaries [6], which form near the old grain boundaries. After 2 and 3 passes of ECAP, the microstructure is further refined by increasing the fraction of fine grains and decreasing the width of deformation bands/elongated grains (seen in Fig. 1c–f). Arrows A and B in Fig. 1d and f will be discussed below. After 4 passes, the microstructure homogeneity has been improved greatly and a high fraction of ultrafine grains is achieved (Fig. 1g).

Fig. 1h shows a high resolution grain boundary map (step size, 50 nm) after 4 ECAP passes. HAGBs (above 15°) are marked with thick black lines. A relatively high fraction of twins {110} ($38.9^\circ \pm 5^\circ$ b110N) is surprisingly observed in the microstructure after 4 passes, which mainly appears near the HAGBs (marked by thick red lines). In

Corresponding author.

E-mail address: happywinner01@gmail.com (Y.J. Chen).

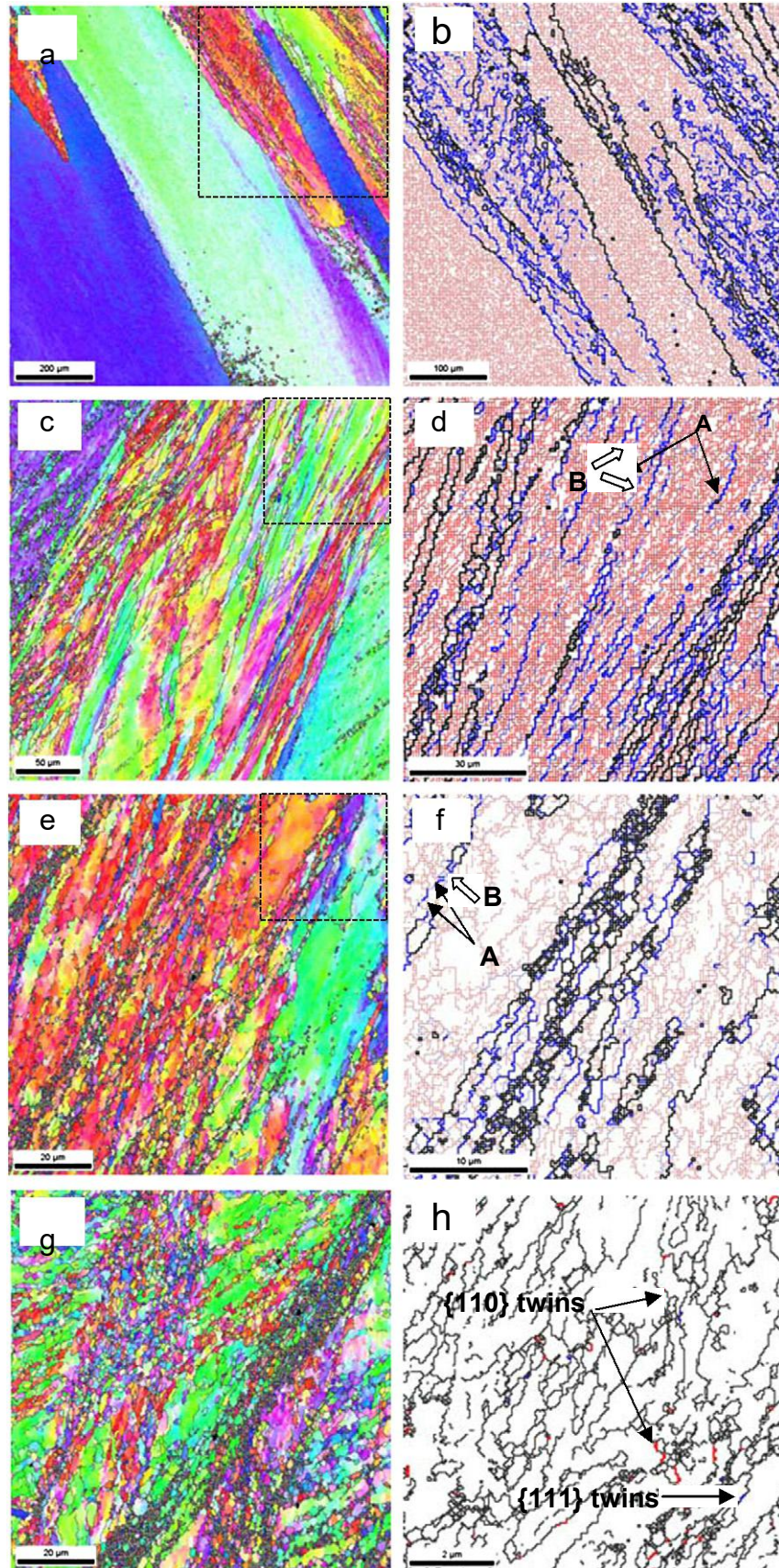


Fig. 1. Orientation maps (left column) and the magnified grain boundary maps (Figs. 1b, d and f) from the dashed square area (left column) of Al-1 wt.% Mg alloy processed by ECAP at cryogenic temperature and (a, b) 1, (c, d) 2, (e, f) 3 and (g) 4 passes, respectively. Fig. 1h showing twins in a high resolution grain boundary map (step size, 50 nm) of 4 passes.

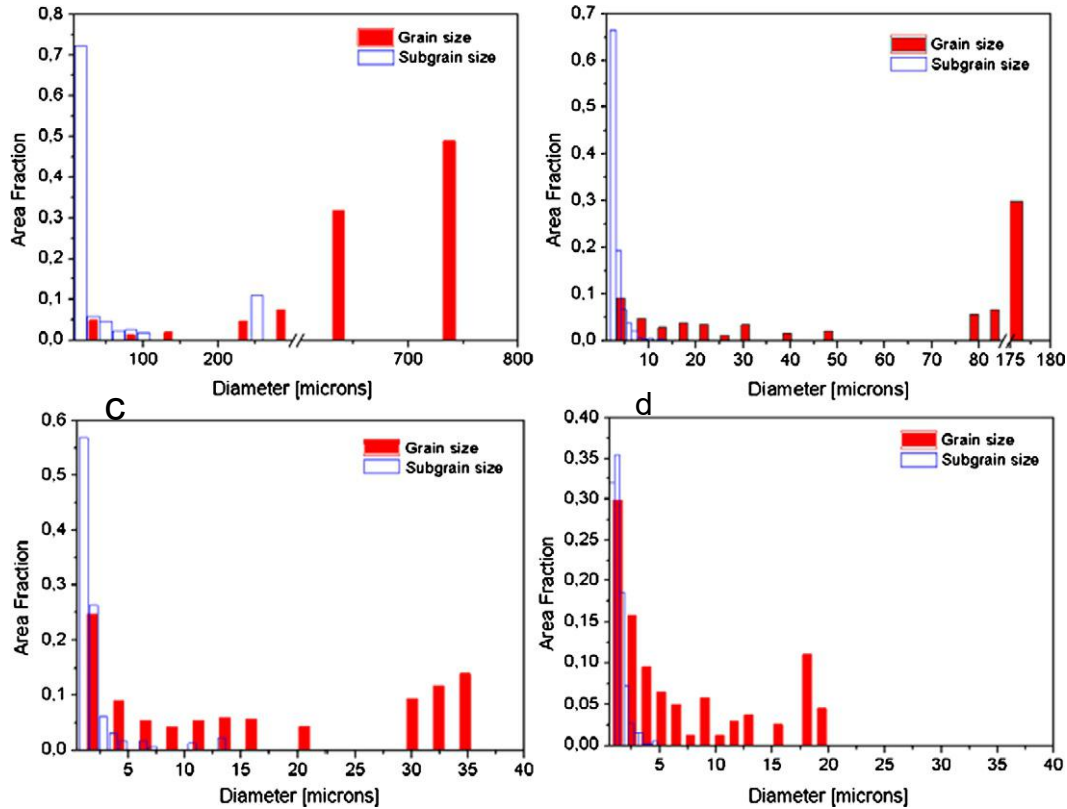


Fig. 2. Grain and subgrain size distributions of Al-1 wt.% Mg alloy processed by ECAP at cryogenic temperature and (a) 1, (b) 2, (c) 3 and (d) 4 passes.

addition, a very small fraction of twins $\{111\}$ ($60^\circ \pm 5^\circ$ b111N) is detected (marked by thick blue lines). Both twins are identified by EBSD software according to the criteria of twins [7]. Twins in Al alloys usually occur in nanocrystalline aluminium [8] or with nano twins in ultrafine-grained aluminium [9]. The occurrence of twins $\{110\}$ and $\{111\}$ with length less than 500 nm is probably induced by the high local stress concentration during ECAP at cryogenic temperature.

Fig. 2 shows the typical distribution histograms of grain and subgrain sizes (equivalent circle diameter) for the images shown in Fig. 1a, c, e and g. The definition of grains and subgrains can be found in Ref [10]. The distribution ranges of both grain and subgrain sizes narrow continuously and the distribution peaks move towards left side with increasing strain (Fig. 2a–d), indicating the mean grain and subgrain sizes are reduced gradually (shown in Table 1).

Aluminium and its alloys have very high rate of dynamic recovery due to their high stacking fault energy [6,11]. Therefore, recovery dominated continuous dynamic recrystallization (CDRX) is expected to be activated during deformation. Actually, CDRX has been observed in Al alloys processed by ECAP at high temperature [12,13]. By contrast, ECAP at cryogenic temperature may greatly suppress the dynamic recovery without the aid of temperature. Therefore, the grain refinement mechanism of Al alloys during ECAP at cryogenic temperature is unclear. CDRX occurs in turn by the progressive accumulation of dislocations in LAGBs, leading to the increase of misorientation and the evolution of LAGBs into HAGBs [6]. The

incomplete new HAGB segments (with misorientation in the range of 15° – 30°), which are frequently observed within grains (examples are marked by arrow A in Fig. 1d and f), are normally connected by LAGBs with higher misorientation in the range of 10° – 15° (examples are marked by arrows B in Fig. 1d and f). This may be the direct evidence of CDRX process that HAGBs evolve from LAGBs by gradually increasing misorientation. Fig. 3a compares the rate of microstructural refinement in present data and the other studies [14–17], where their fraction of HAGBs and mean misorientation are shown as a function of equivalent strain. The minimum misorientation of 2° is used in this figure. Fig. 3a clearly demonstrates a fact that the fraction of HAGBs and misorientation of Al-1 wt.% Mg alloy processed by ECAP at cryogenic temperature increase continuously as equivalent strain increases. This result agrees with the evolution of misorientation and the fraction of HAGBs through CDRX mechanism. In general, two more trends are evident in Fig. 3a. First, the fraction of HAGBs and misorientation at each pass increase sharply by decreasing extrusion temperature, indicating the increase of the rate of grain refinement. Second, misorientation at each pass increases by reducing the initial grain size [14,17]. This means that the rate of grain refinement could increase by using smaller initial grain size.

The progressive rotation of subgrains adjacent to pre-existing grain boundaries, which is induced by strain during CDRX mechanism, results in large misorientation gradient from the center to the edge of old grains [18]. Large misorientation gradients have been observed in hot compressed Al-Mg alloys by TEM [19] and EBSD [20]. However, the microstructure after ECAP, especially processed at cryogenic temperature, is much more complicated. Thus it is interesting to study the mean misorientation gradient statistically. Fig. 3b shows the mean misorientation gradient, from the center to the edge of old grains, as a function of equivalent strain. The gradient measured from two principal orthogonal directions, i.e., parallel to (major axis) and perpendicular to (minor axis) the elongated direction. The misorientation gradients of major and minor axes increase sharply as equivalent strain accumulates

Table 1
Summary of mean grain and subgrain sizes as a function of ECAP pass at cryogenic temperature.

ECAP pass	LAGBs (μm)	HAGBs (μm)
1	10.02	19.76
2	2.41	4.27
3	1.03	1.39
4	1.0	1.33

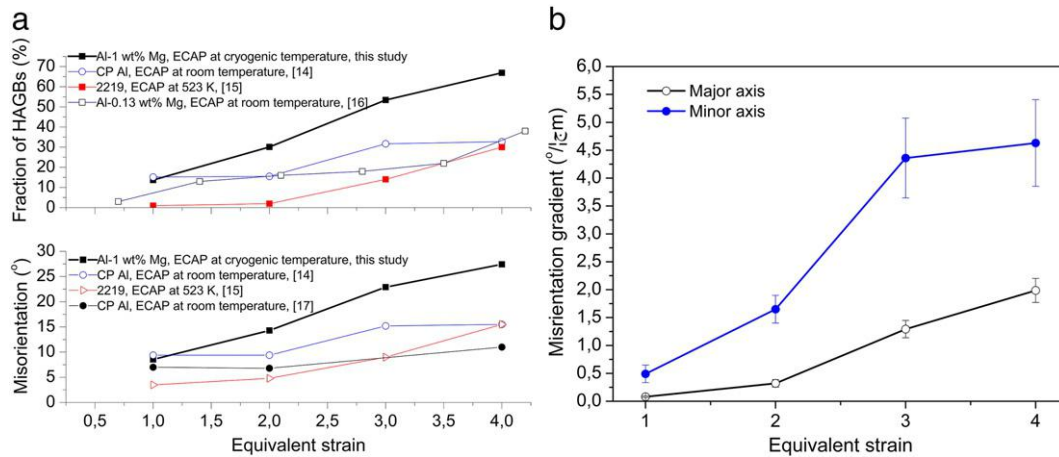


Fig. 3. (a) Fraction of HAGBs and misorientation as a function of equivalent strain and (b) misorientation gradient of Al-1 wt.% Mg alloy processed by ECAP at cryogenic temperature as a function of equivalent strain.

from 1 to 4. The misorientation gradient of minor axis at ECAP 4 passes is $4.6^\circ/\mu\text{m}$, which is 23 times of the same alloy after hot compression [20]. The misorientation gradient of minor axis is significantly higher than the major axis in 1–4 passes of ECAP.

Although the microstructure homogeneity of Al-1 wt.% Mg alloy has been improved greatly with increasing strain (seen in Fig. 1 a, c, e and g), there is obvious evidence for the presence of coarse grains which are not equiaxed and inhomogeneous (seen in Fig. 1g). This observation contrasts with that of Al-1 wt.% Mg alloy processed by ECAP at room temperature [1], where the grains are reasonably equiaxed and homogeneous after four passes. Therefore, an immediate conclusion from this comparison is that lowering extrusion temperature retards, at least partially, the evolution of the equiaxed microstructure. This conclusion agrees with the report by Chen et al. [21], where raising extrusion temperature of ECAP causes grain shape to become more equiaxed in Al alloys. It can be seen from Table 1 that the grain/subgrain size after 4 passes of ECAP at cryogenic temperature seems bigger than the report in Ref [1]. The reasons may be explained as: (a) bigger initial grain size ($960 \mu\text{m}$) is used in this study, (b) bigger geometry of the ECAP die ($20 \times 20 \text{ mm}^2$) is employed, (c) to study the grain refinement quantitatively and precisely, a big representative area ($100 \times 100 \mu\text{m}^2$ in present study) is necessary to be investigated. The conclusion about the mean grain (subgrain) size obtained by TEM from a very small area (seen in Ref [1]) is, therefore, crude.

4. Conclusions

Microstructure evolution of Al-1 wt.% Mg alloy processed by ECAP at cryogenic temperature from 1 to 4 passes has been investigated quantitatively by EBSD. Both mean grain and subgrain sizes are reduced gradually with increasing ECAP pass. ECAP at cryogenic temperature increases the rate of grain refinement by promoting the

fraction of HAGBs and misorientation at each pass. The fraction of HAGBs and the misorientation of Al-1 wt.% Mg alloy after ECAP increase continuously as a function of equivalent strain. Both $\{110\}$ and $\{111\}$ twins at ultrafine-grained size are observed firstly in Al-Mg alloys during ECAP. The analysis on grain boundaries and misorientation gradient demonstrates the grain refinement mechanism of CDRX.

References

- [1] Iwahashi Y, Horita Z, Nemoto M, Langdon TG. *Metall Mater Trans* 1998;29A: 2503–10.
- [2] Morishige T, Hirata T, Uesugi T, Takigawa Y, Tsujikawa M, Higashi K. *Scr Mater* 2011;64:55–8.
- [3] Prangnell PB, Bowen JR, Apps PJ. *Mater Sci Eng A* 2004;375–377:178–85.
- [4] Wang J, Iwahashi Y, Horita Z, Furukawa M, Nemoto M, Valiev RZ, et al. *Acta Mater* 1996;44:2973–82.
- [5] Stolyarov VV, Lapovok R. *J Alloys Compd* 2004;378:233–6.
- [6] Gourdet S, Montheillet F. *Mater Sci Eng A* 2000;283:274–88.
- [7] OIM Analysis 5.3 Software User Manual. EDAX/TSL; 2007.
- [8] Zhu YT, Liao XZ, Srinivasan SG, Zhao YH, Baskes MI, Zhou F, et al. *Appl Phys Lett* 2004;85:5049–51.
- [9] Liu MP, Roven HJ, Yu YD, Werenskiold JC. *Mater Sci Eng A* 2008;483–484:59–63.
- [10] Chen YJ, Li YJ, Walmsley JC, Dumoulin S, Gireesh SS, Armada S, et al. *Scr Mater* 2011;64:904–7.
- [11] Lee DN. *Mater Sci Forum* 2005;495–497:1243–8.
- [12] Sitdikov O, Sakai T, Avtokratova E, Kaibyshev R, Tsuzaki K, Watanabe Y. *Acta Mater* 2008;56:821–34.
- [13] Kaibyshev R, Mazurina I. *Mater Sci Forum* 2004;467–470:1251–60.
- [14] Mazurina I, Sakai T, Miura H, Sitdikov O, Kaibyshev R. *Mater Sci Eng A* 2008;473: 297–305.
- [15] El-Danaf EA. *Mater Sci Eng A* 2008;487:189–200.
- [16] Reihanian M, Ebrahimi R, Moshksar MM, Terada D, Tsuji N. *Mater Charact* 2008;59:1312–23.
- [17] Apps PJ, Bowen JR, Prangnell PB. *Acta Mater* 2003;51:2811–22.
- [18] Humphreys FJ, Hatherly M. *Recrystallization and related annealing phenomena*. second ed. Oxford: Pergamon Press; 2004.
- [19] Drury MD, Humphreys FJ. *Acta Metall* 1986;34:2259–71.
- [20] Ashton MJ, Humphreys FJ. *Mater Sci Forum* 2004;467–470:117–22.
- [21] Chen YC, Huang YY, Chang CP, Kao PW. *Acta Mater* 2003;51:2005–15.